TM-70-2015-3

TECHNICAL MEMORANDUM

ELECTRICAL CONDUCTIVITY AND TEMPERATURE OF THE LUNAR INTERIOR

Bellcomm

BELLCOMM, INC.
955 L'ENFANT PLAZA NORTH, S.W., WASHINGTON, D.C. 20024

COVER SHEET FOR TECHNICAL MEMORANDUM

TITLE- Electrical Conductivity and Temperature of the Lunar Interior

TM-70-2015-3

DATE- September 2, 1970

FILING CASE NO(S)- 340

AUTHOR(S)- W. R. Sill

FILING SUBJECT(S)
(ASSIGNED BY AUTHOR(S))-

ABSTRACT

An analysis of time domain recordings of the lunar surface magnetic field (Apollo 12) has been performed to provide electrical conductivity information to depths of about 300 km. Assuming a dominant poloidal interaction leads to models with conductivities in the range from 3×10^{-3} to 10^{-2} mho/m below 200 km. For a postulated pyroxenite composition of the lunar interior such conductivities correspond to temperatures in the range from 1200 to 1300°K. Other less conductive and cooler models are possible.

BA-145A (8-68)

SEE REVERSE SIDE FOR DISTRIBUTION LIST

DISTRIBUTION

COMPLETE MEMORANDUM TO

CORRESPONDENCE FILES:

OFFICIAL FILE COPY
plus one white copy for each additional case referenced

TECHNICAL LIBRARY (4)

NASA Headquarters
R. J. Allenby/MAL
W. O. Armstrong/MTX
P. E. Culbertson/MT
R. J. Green/MAL
E. W. Hall/MTG
T. A. Keegan/MA-2
R. L. Lohman/MF
M. A. Mitz/SL
W. T. O'Bryant/MAL
A. W. Schardt/SG
L. R. Scherer/MAL
A. D. Schnyer/MTE
J. W. Wild/MTE
NASA Headquarters Library/USS-10

Ames Research Center
D. S. Colburn/SSE
P. Dyal/SSE
D. E. Gault/SSP
W. I. Linlor/SSE
L. Roberts/M (2)
C. P. Sonett/SS (3)
J. R. Spreiter/SST

Goddard Space Flight Center
J. E. Ainsworth/621
S. J. Bauer/615
R. E. Hartle/514
J. P. Heppner/612
G. D. Mead/641
N. F. Ness/512
J. A. O'Keefe/640
C. C. Stephanides/620
D. A. Stern/641
R. G. Stone/615
W. F. Templemon/252
D. J. Williams/611

Jet Propulsion Laboratory
D. R. Clay/183-401
M. Neugebauer/183-401
R. Phillips/183-501
D. Rea/183-401

COMPLETE MEMORANDUM TO

Jet Propulsion Laboratory (Cont'd.)
E. J. Smith/183-401
C. W. Snyder/183-401

Manned Spacecraft Center
A. W. England/CB
C. R. Nicks/FA4
D. W. Strangway

American Nucleonics Corporation
K. Schwartz

Australian National University
E. Essene
A. E. Ringwood

California Institute of Technology
D. Anderson
L. Davis, Jr.
B. C. Murray
E. Shoemaker

Cornell University
T. Gold
C. Sagan

Environmental Science Service Administration/Boulder
W. N. Hess
J. R. Wait

General Dynamics/Astronautics
J. J. Gilvarry

Geological Survey of Canada
A. Larochelle
E. J. Schwartz

Grant Institute of Geology
G. M. Biggar
M. J. O'Hara
S. W. Richardson

Harvard University
C. Frondel

Lamont-Doherty Geological Observatory
M. Ewing
G. V. Latham

DISTRIBUTION LIST (CONT'D.)

Complete Memorandum to

Max-Planck Institut für Extraterrestrische Physik
J. V. Hollweg

Massachusetts Institute of Technology
J. H. Binsack
H. S. Bridge
E. F. Lyon
T. R. Madden
F. Press
M. G. Simmons
G. S. Siscoe
N. Toksoz

National Radio Astronomy Observatory
J. W. Findlay

Princeton University
R. A. Phinney

Rice University
A. J. Dessler
J. W. Freeman
F. C. Michael

Royal Institute of Technology/ Stockholm
H. Alfvén

Stanford University
J. R. Booker
J. Clarebout
R. Kovach

The University, Newcastle-upon-Tyne, England
S. K. Runcorn

TRW Systems, Inc.
F. Scarf

U.S. Department of the Interior
S. F. Singer

U.S. Geological Survey/Flagstaff
R. E. Eggleton
R. Reagan
D. S. Roddy

Complete Memorandum to

U.S. Geological Survey/Menlo Park
R. R. Doell
H. Masursky

University of Alaska
S. I. Akasofu

University of Arizona
G. P. Kuiper
G. Sill

University of California at Berkeley
K. A. Anderson
F. S. Mozer
S. Ward
J. Wilcox

University of California at Los Angeles
P. J. Coleman, Jr.
W. M. Kaula
W. W. Rubey
G. Schubert
G. Wetherill

University of California at San Diego
J. Arnold
H. Urey

University of California at Santa Barbara
P. E. Cloud
G. J. F. MacDonald

University of Colorado
E. E. Larson

University of Iowa
J. A. Van Allen

University of Kansas
D. B. Beard
W. W. Shen

University of Massachusetts
D. U. Wise

University of New Hampshire
L. J. Cahill

University of Sidney
B. O'Brian

University of Texas at Dallas
C. E. Helsley
F. S. Johnson
J. E. Midgley

DISTRIBUTION LIST (CONT'D.)

Complete Memorandum to

University of Tokyo
T. Nagata

Bellcomm, Inc.
D. R. Anselmo
A. P. Boysen, Jr.
J. O. Cappellari, Jr.
F. El-Baz
D. R. Hagner
W. G. Heffron
J. J. Hibbert
N. W. Hinners
T. B. Hoekstra
M. Liwshitz
J. L. Marshall
K. E. Martersteck
J. Z. Menard
G. T. Orrok
P. E. Reynolds
P. F. Sennewald
R. V. Sperry
A. W. Starkey
J. W. Timko
A. R. Vernon
R. L. Wagner
D. B. Wood
All Members Department 2015
Central Files
Department 1024 File
Library

Abstract Only to

Bellcomm, Inc.
J. P. Downs
I. M. Ross
M. P. Wilson

BELLCOMM, INC.
955 L'ENFANT PLAZA NORTH, S.W. WASHINGTON, D. C. 20024

SUBJECT: Electrical Conductivity and Temperature of the Lunar Interior - Case 340

DATE: September 2, 1970

FROM: W. R. Sill

TM70-2015-3

TECHNICAL MEMORANDUM

1.0 INTRODUCTION

Data returned from the Apollo 12 lunar surface magnetometer has shown the presence of a steady field of about 36γ and a fluctuating component of an amplitude that is often considerably larger than that of the fluctuations observed in lunar orbit by Explorer 35, [NASA, 1970]. The steady component is attributed to the remnant magnetization of a large body acquired when the inducing fields were much larger than at present [Dyal et al., 1970a].

When the moon is in the solar wind, the time varying field at the lunar surface consists of the superposition of the interplanetary magnetic source field, the poloidal (eddy current) induced field driven by the time variations in the source field and the toroidal response field due to the motional electric field. An initial analysis of the observed time varying lunar surface field has been in terms of a simple model consisting of a conductive core of about 10^{-4} mho/m surrounded by a nonconductive crust of a thickness on the order of 100 km [Sonett, 1970; Sonett et al., 1970; Monitor, 1970]. If one assumes that the poloidal response is much stronger than the toroidal response, then the above is consistent with the observed transient response time ($\sim$100 sec) to step function changes in the source field and with the amplification ($\sim$5x) of the tangential component of the lunar surface field relative to the interplanetary magnetic field.

A careful examination of the published time domain recordings indicates that the assumed predominance of the poloidal response is probably correct at frequencies above 10^{-2} Hz. Assuming this predominance extends to lower frequencies indicates that some information on the conductivity below 200 km is present in the data. The fact that the poloidal response increases with frequency tends to make the higher frequencies stand out in time domain recordings. Accordingly, there is a tendency to select models which fit the high frequency data and therefore the models are more indicative of the near surface conductivity.

2.0 LUNAR SURFACE MAGNETIC FIELD

Calculations based on various lunar conductivity models have shown that the poloidal response becomes important at frequencies above the inverse of the Cowling time for the most

conductive interior portion [Blank and Sill, 1969a; Sill and Blank, 1969, 1970]. The poloidal response continues to increase with frequency as the outer less conductive regions become inductive and the induced field becomes compressed within the non-inductive crust. On the other hand, the toroidal response for these models is flat at low frequencies and falls off at high frequencies [Blank and Sill, 1969b; Sill and Blank, 1970]. Both the magnitude of the toroidal field and the region of the high frequency cutoff are typically determined by the most resistive crustal layer.

When the poloidal interaction is dominant, the lunar surface magnetic field should appear enriched in the high frequency components, in response to broad band, white noise in the interplanetary field. This effect can be seen in Figure 1 [Dyal, 1970b] which shows a comparison of the lunar surface magnetic field, B(LSM), at the Apollo 12 site and the interplanetary magnetic field, B(IMF), as measured by Explorer 35 in lunar orbit. In general, one notes not only that the horizontal components (y, z) of the lunar surface field are considerably amplified with respect to the parallel component of the interplanetary field, but also that the lunar surface traces appear to be dominated by the higher frequencies. A good example occurs in the record between 32 and 49 minutes, where the z component of the interplanetary field shows an abrupt change in mean level (dashed line) of $\sim$3 units, followed by a quasi-sinusoidal - oscillation with a peak-to-peak amplitude of $\sim$2.7 units. At the lunar surface the abrupt change in mean level ($\sim$6.5 units) - of the parallel component is almost obscured by the large ($\sim$9.6 units) quasi-sinusoidal oscillations.

3.0 LUNAR CONDUCTIVITY MODELS

Simple calculations of the amplification (ratio of the lunar surface field to the interplanetary field) of the principal frequency component in the square wave from 1 to 1', the quasi-sinusoid at 2 and 4 and other fluctuations at the indicated points are shown as circles in Figure 2.

The clustering of the points is a result of the time scale used in the display and the greater amplification of the higher frequencies, which makes the calculation of the gain easiest for frequencies of the order of .01 Hz. Note that the observed gain increases with frequency, indicating a dominant contribution from the poloidal mode at the higher frequencies.

Figure 2 also shows the magnitudes of the poloidal and toroidal transfer functions for several conductivity models. Below .1 Hz, the poloidal response is insensitive to the structure of the outer 100 km, provided the effective conductivity is less than 10^{-5} mho/m. On the other hand, the toroidal response for the models shown is not sensitive to the conductivity below 100 km.

At any given frequency, the gain or ratio of the lunar surface field to the interplanetary field is determined by a weighted sum of the magnitudes of the poloidal and toroidal transfer functions [Sill and Blank, 1969; 1970]. Since the x,y plane is almost parallel to the ecliptic, this ratio for the z or north component is simply

$$\frac{B_z(\text{LSM})}{B_z(\text{IMF})} = \left|H_p\right| + \left|H_t\right| \qquad (1)$$

In order to compare the observed ratios with theoretically derived ones, we must ascertain the contributions from each of the modes. Two-layer model calculations show the toroidal response to be much less than 1, if the conductance per unit area of the surface layer is much less than 10^{-12} mho/m^2. Nagata [1970] reports a conductivity of 10^{-9} mho/m for an Apollo 11 crystalline rock at 300°K, a value which is typical of terrestrial basalts as measured in the laboratory. Simulating the regolith conditions on the lunar surface by vacuum drying and powdering terrestrial basalts gives conductivities in the range from 10^{-13} to 10^{-16} mho/m [Strangway, 1969], so that a few meters of such material at the surface would effectively quench the toroidal response of the moon.

Assuming that the toroidal response is much less than 1, we need then only to compare the observed ratios with the magnitude of the poloidal response. In Figure 2 we see that near 10^{-2} Hz the poloidal response models 1, 2 and 3 provide an adequate fit to the data. This is because they all have a conductivity of 5×10^{-4} mho/m between 100 and 200 km. Within the estimated accuracy ($\sim$15%) of these simple calculations, either model 1 or 2 provides an adequate fit to the lowest frequency point at 5×10^{-4} Hz. Thus, consistent with these two models, a conductivity of the order of 10^{-2} mho/m is permissible below 300 km.

The assignment of a frequency to the observed amplification factors is simply based on the time duration of the fluctuation. For the quasi-sinusoids, this estimate is probably satisfactory but for the lowest frequency event (point 1 in Figure 2) the estimate is only approximate. Instead of an actual spectral decomposition of the records in Figure 1, a better estimate of the low frequency response and deep electrical properties can be made by fitting a model to the data in the time domain.

Figure 3 shows the time domain response of a model (1a) to a simulation of the event in Figure 1 between 1 and 1'. Model 1a is the same as model 1 in the outer 300 km and has a conductivity of 3×10^{-2} mho/m below 300 km. The increase in the core conductivity in model 1a over model 1 was necessary to fit the observed amplification of the mean level ($\sim$2X). Either model 1a or 1 provide an adequate fit to the amplification of the sinusoid.

Note also the general qualitative agreement between the real and simulated events, i.e., the overshoot on the first half of the sinusoid at 1 and the large negative overshoot after the mean level decrease at 1'.

The normalized slope ($B^{-1}\ \partial B/\partial t$) or rate of decay of the negative overshoot increases from about 30 sec near the peak to about 300 sec after about 50 sec. This is a manifestation of the different rates of decay for the various frequency components that are associated with the end of the square wave at 1'. The higher frequency components have smaller skin depths and therefore decay at a faster rate. The smaller skin depths of the higher frequencies also mean that they sample the less conductive layers closer to the lunar surface. For this reason one must be careful in the time domain interpretation of decay curves associated with step function changes in the field. A simple exponential decay interpretation of the first 50 sec of the overshoot decay of Figure 3 would give a time constant of 55 sec which corresponds to the Cowling decay time for a sphere of radius 1.64×10^{3} km and a conductivity of 2×10^{-4} mho/m. This conductivity is a serious underestimate of the maximum interior conductivity (3×10^{-2} mho/m) of this model.

A lower limit for the interior conductivity can be obtained by determining the maximum effect of a non-zero toroidal response, assuming that at the lowest frequency (5×10^{-4} Hz), the poloidal transfer function has its smallest value, $|H_p| = 1$. Then, since the total observed ratio is 2, the maximum value for the toroidal response is $|H_t| = 1$. Subtracting this maximum value from the observed ratios gives the values of H_p indicated by crosses. A model (4) with an interior conductivity of 2.5×10^{-4} mho/m provides an adequate fit to these data.

4.0 LUNAR TEMPERATURES

Inferences on the temperature based on the conductivity models are complicated by our lack of knowledge of the composition of the lunar interior. Figure 4 shows the conductivity-temperature relations for several terrestrial rocks (basalt, pyroxenite,

olivine-pyroxenite, [Parkhomenko, 1967]) and minerals (olivine, [England et al., 1968]), the Earth's mantle [Swift, 1967] and an Apollo 11 crystalline (basaltic) rock [Nagata, 1970]. Also indicated are the conductivities and depths from models 1 to 4.

Olivine, which has been used as a model for the electrical conductivity of a chondritic Moon [England et al., 1968], is much less conductive than terrestrial basalt or the Apollo 11 basalt, as was pointed out by Nagata [1970]. A basalt model for the Moon will thus lead to lower temperatures than olivine. However, basalt cannot represent the mean lunar composition, because this will lead to an excessively dense Moon [Ringwood and Essene, 1970].

Pyroxenite has been suggested as a plausible material for the composition of the lunar interior [O'Hara et al., 1970; Ringwood and Essene, 1970]. The two curves shown for a pyroxenite and an olivine-pyroxenite indicate that material of this composition is less conductive than olivine at temperatures below 1300°K, and will therefore lead to higher temperatures for any given conductivity.

The three most conductive models (1, 1a and 2) and the olivine and pyroxenite curves give rise to temperatures in the range from 1000°K to 1200°K for the layer from 200 km to 300 km and temperatures about 1200°K to 1400°K below 300 km. The least conductive models (3 and 4) correspond to temperatures below 100 km in the range from 850°K to 900°K for olivine and 1000°K for pyroxenite. With the Apollo 11 basalt relationship all the poloidal models could be accommodated with temperatures below 750°K.

The most conductive models (1 and 1a) and the pyroxenite relation give rise to temperatures which are 500°K below the pyroxenite solidus at 100 km and about 300°K below the solidus at 300 km [Ringwood and Essene, 1970]. Whether such temperatures are compatible with the strength needed to support the mascons is a problem which needs to be investigated.

5.0 SUMMARY

Lunar models with conductivity of the order of 10^{-2} mho/m below 300 km are compatible with the data, assuming that the toroidal response is negligible. Furthermore, assuming olivine or pyroxenite as representative of the composition of the lunar interior, this conductivity corresponds to temperatures of about 1200°K to 1400°K. Taking into account the maximum possible effect of a toroidal response gives results which are compatible with a conductivity of 2×10^{-4} mho/m below 100 km. This figure is equivalent to the olivine and pyroxenite conductivities at 850°K and 1050°K, respectively.

Lower frequency calculations, preferably carried out in the frequency domain [Sill and Blank, 1969, 1970], can unambiguously determine the contribution from the toroidal mode and improve the models for the conductivity (and temperature) of the lunar interior.

W. R. Sill

2015-WRS-gmr

W. R. Sill

Attachments
References
Figures 1-4

REFERENCES

Blank, J. L., and W. R. Sill, Response of the Moon to the Time-Varying Interplanetary Magnetic Field, J. Geophs. Res., 74, 736, 1969a.

Blank, J. L., and W. R. Sill, Reply, J. Geophs. Res., 74, 5175, 1969b.

Dyal, P., C. W. Parkin, and C. P. Sonett, Apollo 12 Magnetometer: Measurement of a Steady Magnetic Field on the Surface of the Moon, Science, 169, 762, 1970a.

Dyal, P., C. W. Parkin, and C. P. Sonett, Lunar Surface Magnetometer Experiment, NASA SP-235, 55, 1970b.

England, A. W., G. Simmons, and D. Strangway, Electrical Conductivity of the Moon, J. Geophs. Res., 73, 3219, 1968.

Monitor, New Scientist, April 16, 1970.

Nagata, T., Electrical Conductivity and Age of the Moon, paper M. 14) presented at Thirteenth Plenary Meeting, COSPAR, Leningrad, USSR, May, 1970.

NASA, Apollo 12 Mission Report, MSC-01855, 3-13, 1970.

O'Hara, M. J., G. M. Biggar, and S. W. Richardson, Experimental Petrology of Lunar Material: The Nature of Mascons, Seas, and the Lunar Interior, Science, 167, 605, 1970.

Parkhomenko, E. K., Electrical Properties of Rocks, Plenum, New York, 1967.

Ringwood, A. E., and E. Essene, Petrogenesis of Lunar Basalts and the Internal Constitution and Origin of the Moon, Science, 167, 607, 1970.

Sill, W. R., and J. L. Blank, Method for Estimating the Electrical Conductivity of the Lunar Interior, Bellcomm TR-69-103-7-4, Bellcomm, Inc., Washington, D.C., 1969.

Sill, W. R., and J. L. Blank, Method for Estimating the Electrical Conductivity of the Lunar Interior, J. Geophs. Res., 75, 201, 1970.

Sonett, C. P., Electrical Conductivity of the Moon: Recent Results, paper presented at NATO Advanced Study Institute on the Moon and the Planets, University of Newcastle upon Tyne, April, 1970.

Sonett, C. P., P. Dyal, and C. W. Parkin, The Apollo 12 Magnetometer: a Progress Report, Trans. Am. Geophs. Union, 50, 349, 1970.

Strangway, D. W., Moon: Electrical Properties of the Uppermost Layers, Science, 165, 1012, 1969.

References (Continued)

Swift, C. M., A Magnetotelluric Investigation of an Electrical Conductivity Anomoly in the Southwestern United States, Ph.D. thesis, Department of Geology and Geophysics, Massachusetts Institute of Technology, July, 1967.

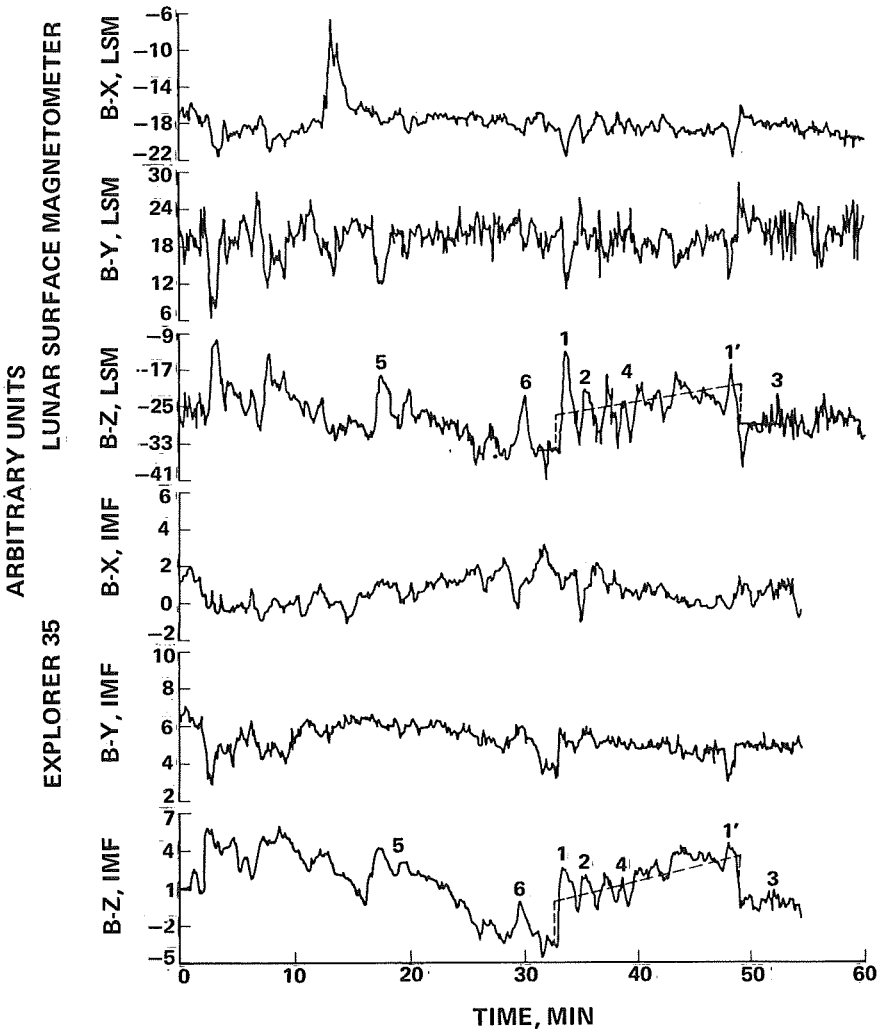

FIGURE 1 - COMPARISON OF THE MAGNETIC FIELD AS SEEN BY EXPLORER 35 IN LUNAR ORBIT AND AT THE LUNAR SURFACE (DYAL ET AL., 1970B).

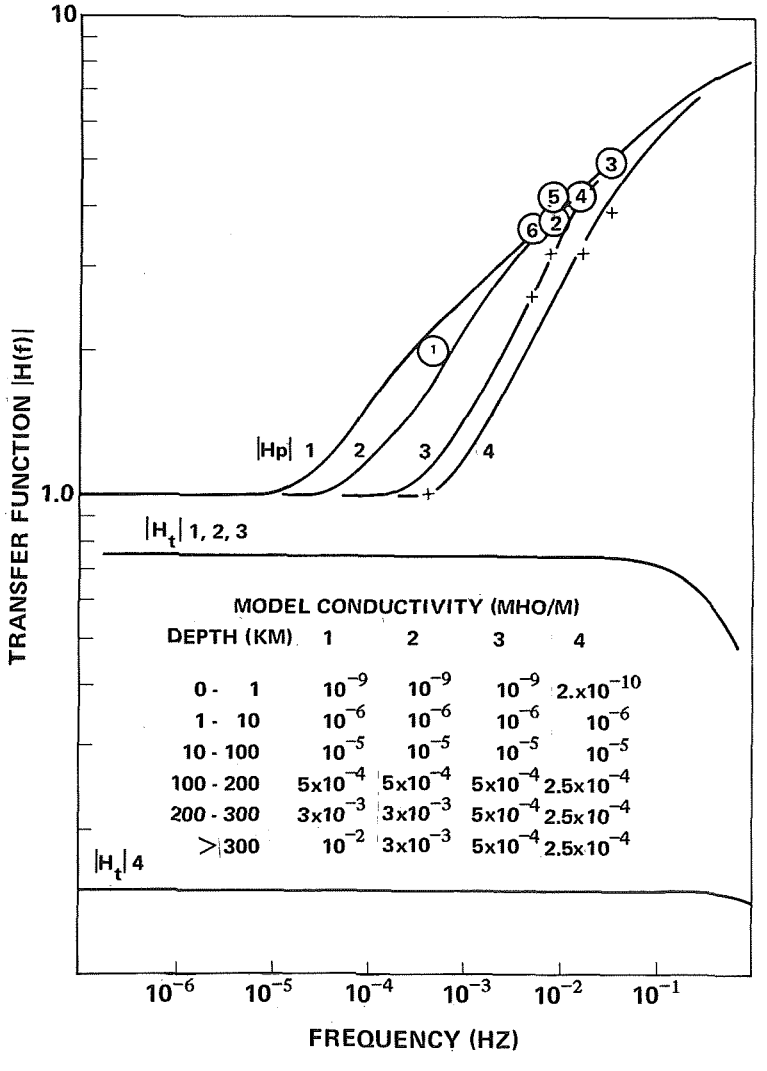

FIGURE 2 - POLOIDAL (H_p) AND TOROIDAL (H_t) TRANSFER FUNCTIONS FOR FOUR LUNAR CONDUCTIVITY MODELS. THE CIRCLES ARE AMPLIFICATION FACTORS, B(LSM/B(IMF), CALCULATED FROM THE FLUCTUATIONS INDICATED IN FIGURE 1.

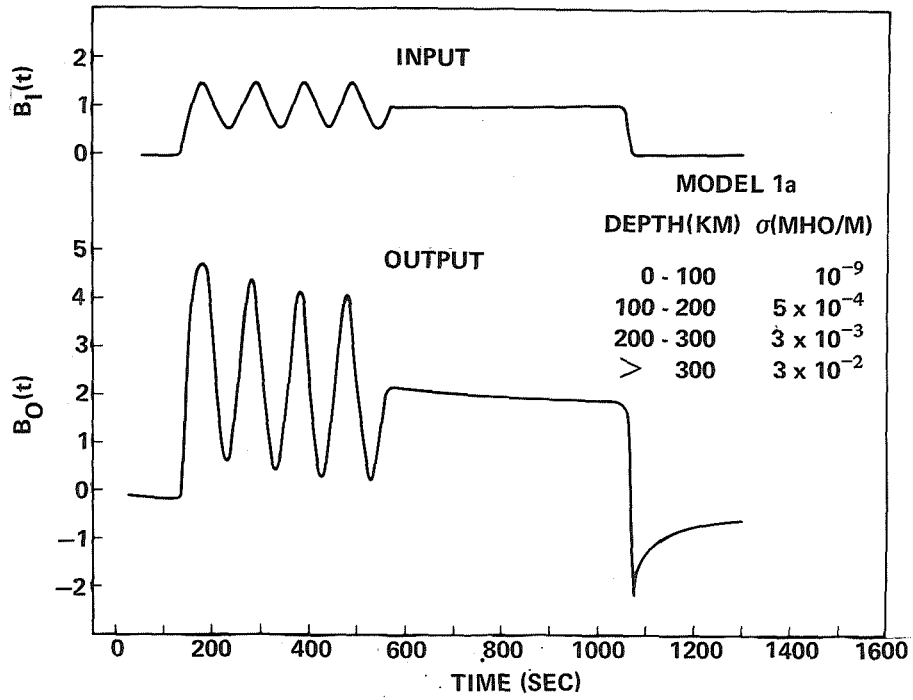

FIGURE 3 - THE TIME DOMAIN RESPONSE, $B_o(t)$, OF MODEL I A TO THE INPUT, $B_I(t)$. THIS IS DERIVED BY COMPUTING THE SPECTRUM OF THE INPUT, $B_I(\omega)$, AND MULTIPLYING BY THE MODEL TRANSFER FUNCTION, $H_p(\omega)$, AND TRANSFORMING THE PRODUCT BACK INTO THE TIME DOMAIN.

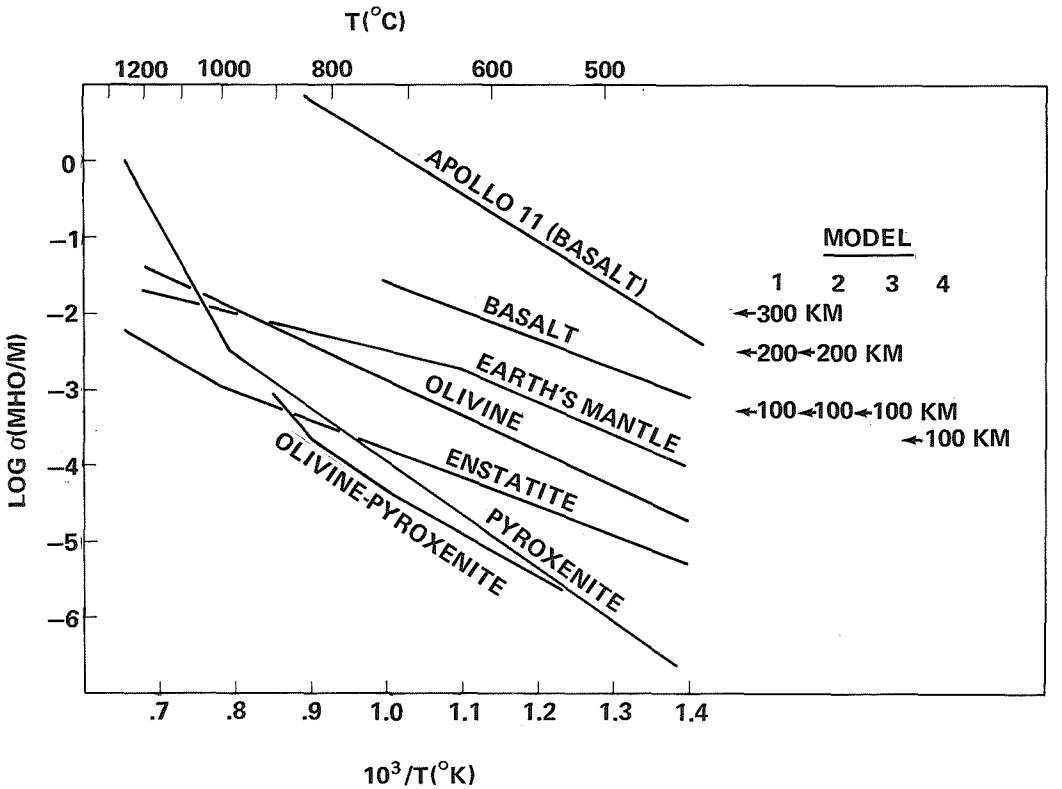

FIGURE 4 - CONDUCTIVITY AS A FUNCTION OF TEMPERATURE FOR TERRESTRIAL ROCKS AND MINERALS AND AN APOLLO 11 CRYSTALLINE ROCK. ALSO SHOWN ARE THE MODEL CONDUCTIVITIES AT THE INDICATED DEPTHS.